Fuel 118 (2014) 1–8

Contents lists available at ScienceDirect

Fuel

journal homepage: www.elsevier.com/locate/fuel

Ignition of methane with hydrogen and dimethyl ether addition

Peng Dai [a], Zheng Chen [a,b,*], Shiyi Chen [a]

[a] SKLTCS, Department of Mechanics and Aerospace Engineering, College of Engineering, Peking University, Beijing 100871, China
[b] Department of Aeronautics and Astronautics, College of Engineering, Peking University, Beijing 100871, China

HIGHLIGHTS

- Ignition enhancement of CH_4 by H_2 and DME addition is studied.
- Different ignition enhancement trends are found for H_2 and DME addition.
- The kinetic effects and transport effects on the ignition enhancement are examined.
- The non-premix ignition is greatly affected by the mass diffusivity of each fuel.

ARTICLE INFO

Article history:
Received 6 September 2013
Received in revised form 20 October 2013
Accepted 22 October 2013
Available online 4 November 2013

Keywords:
Methane/hydrogen
Methane/DME
Ignition
Preferential mass diffusion
Strain rate

ABSTRACT

Premixed and non-premixed ignition of methane/hydrogen and methane/dimethyl ether (DME) binary fuel blends with hot air is studied through numerical simulation with detailed chemistry and variable thermodynamic and transport properties. The emphasis is spent on assessing the kinetic and transport effects involved in CH_4 ignition enhancement caused by H_2 and DME addition. Two configurations are considered: a premixed homogeneous configuration to examine the chemical kinetics and a non-premixed counterflow configuration to assess the transport effects. For the homogeneous ignition process, small amount of DME addition is found to be more effective than H_2 addition in terms of promoting the ignition of CH_4/air mixture. Sensitivity analysis and reaction path analysis are conducted and key elementary reactions involved in CH_4 ignition enhancement by H_2 and DME addition are identified. For the non-premixed ignition process, H_2 addition is shown to be always more effective than DME addition in terms of CH_4 ignition enhancement. It is found that the preferential mass diffusion of H_2 over CH_4 and that of CH_4 over DME have great influence on the local blending ratio at the ignition kernel, which controls the non-premixed ignition process. Therefore, non-premixed ignition of binary fuel blends is significantly affected by the mass diffusivity of each fuel component. Moreover, the effects of strain rate on the non-premixed ignition of CH_4/H_2 and CH_4/DME binary fuel blends with hot air are discussed.

1. Introduction

Due to the rapid increase in energy consumption and increasingly stringent emission regulations, it has become imperative to develop alternative fuels and high-efficiency, low-emission combustion devices [1]. As the cleanest fossil fuel, natural gas (NG) has huge reserves around the world [2]. Recently, natural gas has become one of the most promising alternative fuels because of its favorable chemical characteristics, such as high H/C ratio, large octane number [3], excellent knock resistance [4], and low emissions. However, due to its stable molecular structure, methane (the main component of natural gas) has some unfavorable burning properties such as long ignition delay time, low flame speed, low ignitability, and narrow flammability limit range, which pose great challenges for its utilization in combustion engines. An effective way to solve this problem is to add more reactive fuels such as hydrogen or dimethyl ether (DME) into natural gas to promote its ignition and combustion performance. Therefore, a thorough understanding of fundamental combustion properties of natural gas with hydrogen-like fuel addition is important for developing advanced NG-based combustion engines and corresponding operating strategies.

In the literature, there are many studies on the fundamental combustion properties of CH_4/H_2 or CH_4/DME binary fuel blends, including their ignition delay time [5–8], internal combustion engine (ICE) performance [9–12], laminar flame speed [13–19] and so on. For examples on ignition, Zhang et al. [7] conducted shock-tube experiments to measure the ignition delay time of lean $CH_4/H_2/Ar$ mixtures and they found that the ignition delay time of CH_4/H_2 binary fuel blends has complex dependence on

---

* Corresponding author at: SKLTCS, Department of Mechanics and Aerospace Engineering, College of Engineering, Peking University, Beijing 100871, China. Tel.: +86 10 62766232.

E-mail address: cz@pku.edu.cn (Z. Chen).

0016-2361/$ - see front matter © 2013 Elsevier Ltd. All rights reserved.
http://dx.doi.org/10.1016/j.fuel.2013.10.048

pressure and there exists two-step transition in the global activation energy; Tang et al. [8] measured the ignition delay time of CH_4/DME over a wide range of temperature and pressure and the nonlinear effect of DME addition in ignition promotion was observed and interpreted through kinetic analysis. All the previous studies showed that both H_2 and DME addition can greatly promote the ignition of CH_4. Since the DME oxidation mechanism is totally different from that of H_2, it is expected that the ignition enhancement by adding DME to CH_4 is different from that by adding H_2 to CH_4. Moreover, the kinetics involved in the ignition enhancement should be different for H_2 and DME addition. Therefore, the first objective of this study is to compare different ignition enhancement behavior and identify the kinetics involved in ignition enhancement caused by H_2 and DME addition to CH_4.

Most of previous studies on the transient ignition process of CH_4/H_2 or CH_4/DME were conducted in a homogeneous system, in which only the chemical kinetics during ignition can be thoroughly examined. However, in practical combustion process, ignition usually takes place in non-homogeneous zones due to a lack of time for fully mixing of fuel and air. A laminar non-premixed counterflow configuration can provide a well-defined flow field in which the influence of strain rate, diffusive and convective transports, and their coupling effects with chemical kinetics on ignition can be examined [5,20–24]. For examples, Fotache et al. [22] investigated the forced ignition of CH_4/H_2 blends by hot counter-flowing air and three ignition regimes in terms of H_2 blending ratio were identified; Chen et al. [5] studied the transient ignition of CH_4/DME blends in non-premixed counterflow configuration and they found that the ignition enhancement by DME addition to CH_4 is strongly affected by the strain rate. Other studies using counterflow configuration include premixed ignition of H_2/air by Zheng et al. [23], non-premixed ignition of n-decane/toluene binary fuel blends by Dai et al. [20], and non-premixed ignition of methane with pulsed discharge by Sun et al. [24]. The non-premixed ignition is controlled not only by the chemical kinetics but also the transport of heat and mass. The ratio among the mass diffusivities of H_2, CH_4, and DME is about 6:2:1. Consequently, it is expected that due to the different transport properties, the non-premixed ignition of CH_4 is differently affected by H_2 addition and DME addition. As shown later, the preferential mass diffusion between different fuels in fact plays a very import role in non-premixed ignition. Therefore, the second objective of this study is to compare different ignition enhancement behavior and analyze the transport effects on non-premixed ignition enhancement caused by H_2 and DME addition to CH_4.

Premixed and non-premixed ignition of CH_4/H_2 and CH_4/DME binary fuel blends with hot air is numerically studied in the present work and the chemical kinetics and transport effects involved in the ignition are examined. In order to assess the kinetic effects involved in CH_4 ignition enhancement by H_2 and DME addition, we study the homogeneous ignition process of CH_4/H_2/air and CH_4/DME/air mixtures which is purely controlled by chemical kinetics. In order to examine the transport effects on the ignition of these binary fuel blends, the non-premixed counterflow configuration is employed to study the transient ignition process of CH_4/H_2 and CH_4/DME binary fuel blends with hot air. The rest of the paper is organized as follows. The numerical models and chemical mechanism are introduced in the next section. In Section 3, the homogeneous ignition process of CH_4/H_2 and CH_4/DME binary fuel blends is studied and the kinetic effects involved in CH_4 ignition enhancement by H_2 and DME addition are assessed. In Section 4, the non-premixed ignition process is investigated and the transport effects involved in ignition enhancement are examined using the non-premixed counterflow configuration. Finally, the conclusions are presented in Section 5.

2. Numerical models and chemical mechanism

Since the homogenous ignition process does not have mass or heat transport and is purely controlled by chemical kinetics, we study the adiabatic homogeneous ignition process at constant pressure so that the kinetics involved in CH_4 ignition enhancement by H_2 and DME addition can be revealed. Stoichiometric CH_4/H_2/air and CH_4/DME/air mixtures initially at T_0 = 1400 K and atmospheric pressure are considered and detailed chemistry is employed in simulation. The blending ratio, c, defined as the molar fraction of H_2 or DME in the binary fuel blends, changes from 0 (pure CH_4) to 1.0 (pure H_2 or DME).

In order to examine the transport effects, we study the non-premixed ignition in a counterflow configuration. The transient non-premixed ignition process is simulated using the code for unsteady counterflow flame [25]. The counter-flowing fuel jet is at 300 K and it consists of CH_4/H_2 or CH_4/DME binary fuel blends with the blending ratio of H_2 or DME in the range of $0 \leqslant c \leqslant 1$. The hot air jet is at 1400 K. The pressure is fixed to be P = 1 atm. The distance between the fuel and oxidizer exits is fixed at L = 10 cm. The initial temperature and species distributions are determined under a frozen flow constraint with all the reaction terms suppressed. At the beginning (i.e. t = 0 s), chemical reactions are allowed in the pre-calculated frozen flow field and the afterwards evolution of the reactive counterflow system is simulated. Potential counterflow is considered and thereby the strain rate, a, is given as input parameter in the initial frozen flow, defined as the global gradient of the axial velocity, namely $a = (u_L - u_R)/L$, with the subscripts L and R denoting the fuel (left) and oxidizer (right) jets, respectively. It is noted that increasing strain rate leads to the decrease of flow residence time within ignition kernel, which influences the ignition process in counterflow configuration. Similar procedures were used in previous studies [5,20,26].

In the literature there are few mechanisms that can accurately predict the ignition of both CH_4/H_2 and CH_4/DME binary fuel blends. Here we use the detailed chemical mechanism for DME oxidation developed by Zhao et al. [27]. It consists of 55 species and 290 elementary reactions and was validated against experimental data of ignition delay time from shock-tube, species profiles from flow-reactor, and laminar flame speeds from spherical- and stagnation-flame experiments for DME [27]. Since this DME mechanism contains the H_2 oxidation sub-mechanism developed by Li et al. [28], the ignition process of H_2 as well as DME can be well predicted by this mechanism. In the Supplementary Material we demonstrate that this mechanism against experiments can well predict the ignition delay time of CH_4/DME/air mixtures [8] and CH_4/H_2/air mixtures [7].

3. The homogeneous ignition process

The homogeneous ignition process is studied in order to compare different ignition enhancement behavior and to identify the kinetics involved in ignition enhancement caused by H_2 and DME addition to CH_4. Fig. 1 shows the ignition delay time, τ, of stoichiometric CH_4/H_2/air and CH_4/DME/air mixtures as a function of the blending ratio, c. The ignition delay time is defined as the time when the temperature exceeds its initial value by 400 K (i.e. $T = T_u + 400$ K = 1800 K). Other definitions based on the maximum temperature changing rate and the sudden rise in OH concentration are checked and the ignition delay times defined in different ways are nearly the same (the relative difference is within 2%, see Fig. 1 of Zhao et al. [29]). Fig. 1 indicates that both H_2 and DME addition can greatly reduce the ignition delay time of CH_4/air mixture. However, different enhancing trends are observed for these two additives: the logarithmic ignition delay time of

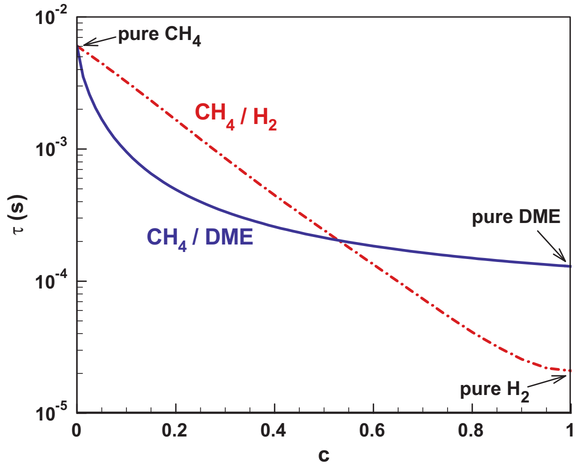

Fig. 1. Change of the homogeneous ignition delay time with the blending ratios of H_2 and DME for stoichiometric CH_4/H_2/air and CH$_4$/DME/air mixtures initially at $T_0 = 1400$ K and $P = 1$ atm.

CH_4/H_2/air changes almost linearly with the H_2 blending ratio; while nonlinear change is observed for CH_4/DME/air (similar trend was observed in shock-tube experiments by Tang et al. [8]). At low DME blending ratio ($0 \leqslant c \leqslant 0.2$), the ignition delay time is greatly reduced by DME addition. However, at high DME blending ratio ($0.4 \leqslant c \leqslant 1$), a further increase of DME blending has little influence on the ignition delay time. Moreover, it is observed that when the blending ratio is below 0.53, DME addition is more effective than H_2 addition in terms of promoting the homogeneous ignition of CH_4/air mixture. (It is noted that the blending ratio is defined based on the molar/volumetric fraction, not the mass fraction.)

Fig. 2a and b respectively show the temporal evolution of radical pool (sum of H, O, OH, CH_3, and HO_2) as well as the specific radical CH_3 at different levels of H_2 and DME blending. Fig. 2a indicates that the radical pool increases almost linearly with the H_2 blending ratio. However, Fig. 2b shows that DME addition has a magnificent boosting effect on radical build-up at small amount of DME addition while such effect is reduced rapidly as the DME blending ratio further increases. Since radical accumulation and run-away determine the ignition process, the difference between ignition enhancement by H_2 and DME addition observed in Fig. 1 can be accounted for by the different impact of H_2 and DME addition on the radical pool development.

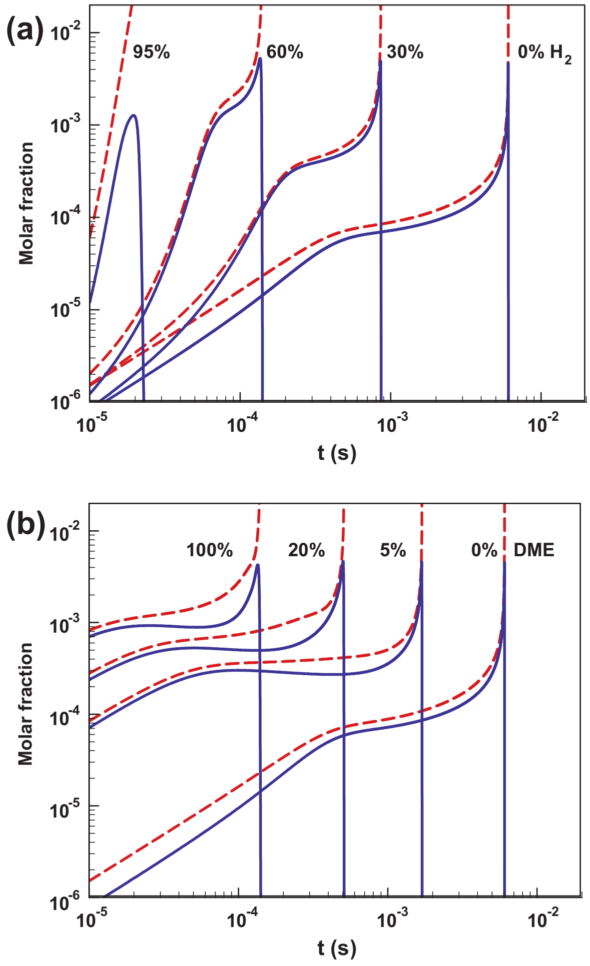

Fig. 2. Temporal evolution of molar fraction of the radical pool (sum of H, O, OH, CH_3 and HO_2, dashed lines) and CH_3 radical (solid lines) during the homogeneous ignition of stoichiometric (a) CH_4/H_2/air and (b) CH_4/DME/air mixtures.

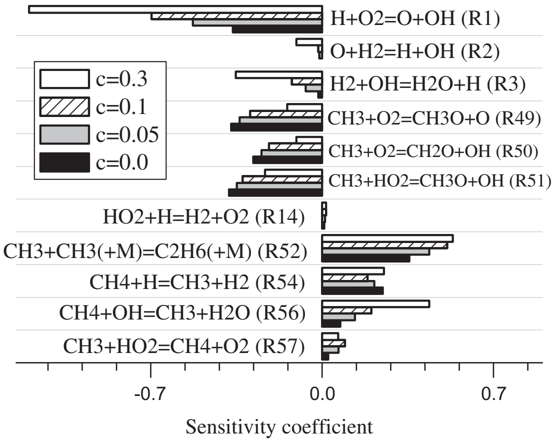

Fig. 3. Sensitivity of key elementary reactions during the homogeneous ignition of stoichiometric CH_4/H_2/air at different levels of H_2 addition.

To identify key elementary reactions involved in CH_4 ignition enhancement by H_2 and DME addition, sensitivity analysis is conducted. The sensitivity coefficient of the ignition delay time with respect to the reaction rate of the ith elementary reaction is defined as:

$$S_i = 10 \cdot \frac{\tau(1.1k_i) - \tau(k_i)}{\tau(k_i)} \tag{1}$$

where $\tau(1.1k_i)$ represents the ignition delay time with the rate constant of the ith reaction being artificially modified to be 1.1 times of its original value, while $\tau(k_i)$ is the original ignition delay time when all reaction rates remain unchanged. The results of sensitivity analysis are plotted in Fig. 3 for different H_2 blending ratios. It is well known that the ignition of CH_4/air is controlled by the slow oxidation of methyl through reactions $CH_3 + O_2 = CH_3O + O$ (R49) and $CH_3 + O_2 = CH_2O + OH$ (R50) [5,22]. Fig. 3 shows that when H_2 is added to CH_4/air mixture, the sensitivity coefficients for reactions (R49) and (R50) as well as that for $CH_3 + HO_2 = CH_3O + OH$ (R51) decrease. On the other hand, sensitivity coefficients for the chain-branching reactions, $H + O_2 = O + OH$ (R1) and $O + H_2 = H + OH$ (R2) and chain-propagation reaction $H_2 + OH = H_2O + H$ (R3) are shown to increase significantly with H_2 blending ratio. Therefore, it is the H_2-related chain reactions (R1–R3) that greatly enhance the radical pool build-up and thereby accelerate the ignition process. Similar observation was also confirmed by Zhang et al. using other detailed chemical mechanisms for CH_4/H_2 binary fuel blends [7].

In order to further explore the kinetics and key elementary reactions involved in the ignition enhancement by H_2 addition, reaction path analysis for radicals such as H, OH, and CH_3 is conducted at different levels of H_2 addition. The contribution of the *i*th reaction to the concentration change of a certain intermediate species *M* is defined as [30]

$$C_{M,\,i} = f_{M,\,i} / \sum_{i=1}^{N} (|f_{M,\,i}|) \qquad (2)$$

where $f_{M,i}$ represents the rate of change in the concentration of species *M* due to the *i*th reaction, and *N* is the total number of elementary reactions. A positive/negative value of $C_{M,i}$ indicates that *M* is produced/consumed by the *i*th reaction. It is noted that only the comparison among values of $C_{M,i}$ for different reactions at the same time is meaningful since the reaction rates change greatly with time during the ignition process. Fig. 4 shows contributions of main elementary reactions to the concentration change of H radical at three different H_2 blending ratios: $c = 0$, 0.05 and 0.3. As the amount of H_2 addition increases, reaction $H_2 + O_2 = HO_2 + H$ (reverse R14) gradually replaces reaction $CH_4(+M) = CH_3 + H(+M)$ (reverse R53) as the main chain-initiation reaction producing H radical. In the late stage of ignition, reaction $H_2 + OH = H_2O + H$ (R3) is shown to be a more important source of H radical while reaction $CH_3O + M = CH_2O + H + M$ (R71) becomes less important. Transition between these two reactions implies that the main path of producing H radical changes from CH_3/CH_3O/CH_2O-relevant reactions to H_2-revelant ones (which have much higher reaction rates) when the level of H_2 addition is increased. Fig. 4 also demonstrates that H_2 addition significantly decreases the portion of reaction $CH_4 + H = CH_3 + H_2$ (R54) in H consumption, and meanwhile makes the chain-branching reaction $H + O_2 = O + OH$ (R1) a more important H sink, which substantially benefits the ignition. Similar reaction path analysis for OH radical is also conducted and the results indicate that reaction $H_2 + OH = H_2O + H$ (R3) gradually replaces $CH_4 + OH = CH_3 + H_2O$ (R56) as an important OH sink when H_2 blending ratio increases. This helps to promote ignition since H radical is much more reactive than CH_3 radical.

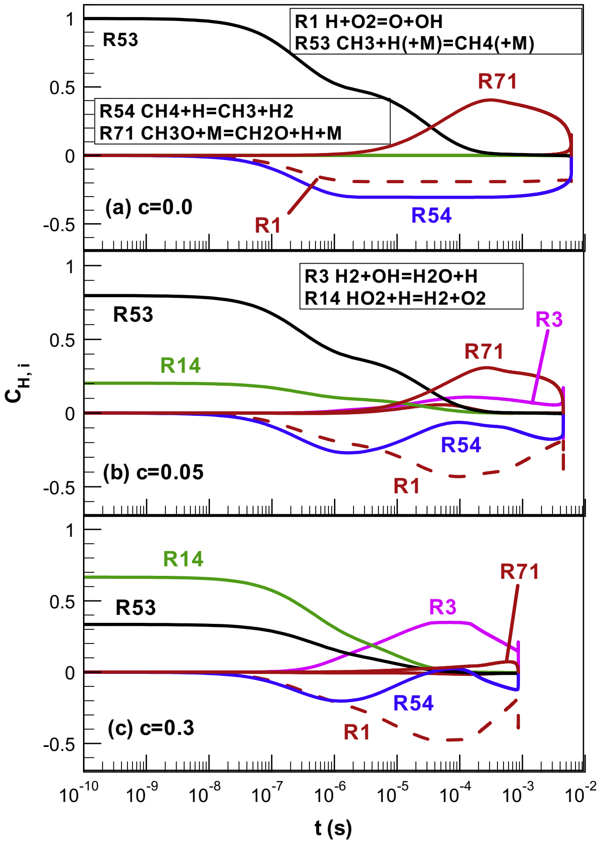

Fig. 4. Contributions of main elementary reactions to the production/consumption of H radical during the homogeneous ignition of stoichiometric CH_4/H_2/air mixture: (a) $c = 0.0$, (b) $c = 0.05$ and (c) $c = 0.3$.

The kinetics involved in CH_4 ignition enhancement by DME addition is also investigated with sensitivity analysis and reaction path analysis. Fig. 5 shows the sensitivity analysis results for the homogeneous ignition of stoichiometric CH_4/DME/air mixtures at different levels of DME addition. It is found that unlike H_2 addition, DME addition benefits the ignition of CH_4 mainly via the unimolecular decomposition reaction $CH_3OCH_3 = CH_3 + CH_3O$ (R239) and the CH_3 oxidation reaction $CH_3 + HO_2 = CH_3O + OH$ (R51), instead of chain reactions (R1–R3) for H_2 addition. The chemical path analysis shows that once a small amount of DME is present, the system is strongly driven by the unimolecular decomposition of DME thorough reaction R239. This reaction is the major initial source of radicals and continues to contribute to radical production thereafter [5]. After DME is decomposed into CH_3 and CH_3O via reaction R239, subsequent H-abstraction reaction $CH_3OCH_3 + CH_3 = CH_3OCH_2 + CH_4$ (R244) produces CH_3OCH_2 which in turn yields additional radical growth through the decomposition reaction $CH_3OCH_2 = CH_2O + CH_3$ (R247). Therefore, with DME addition to CH_4, the radical pool grows rapidly. More importantly, the above reaction sequences produce a large amount of HO_2, which in turn promotes the fast reaction $CH_3 + HO_2 = CH_3O + OH$ (R51) in competition against the much slower counterpart $CH_3 + O_2 = CH_3O + O$ (R49).

To demonstrate the influence of DME and H_2 addition on this competition, Fig. 6 shows the ratio of integral CH_3 consumption through reaction R51 to that through reaction R49 in the homogeneous ignition of stoichiometric CH_4/H_2/air and CH_4/DME/air mixtures. It is seen that the replacement of reaction R49 by R51 for DME addition increases greatly with the blending ratio and it is stronger than that for H_2 addition. Therefore, as shown in Fig. 1, a small amount of DME addition is more effective than H_2 addition in terms of promoting the homogeneous ignition of CH_4/air mixture. (The vertical axis of Fig. 6 is in logarithmic scale which is similar to the ignition delay time shown in Fig. 1.) More details of the comparison between ignition enhancement mechanism of small amount of H_2 addition and that of DME addition are shown in the Supplementary Material accompanying this paper.

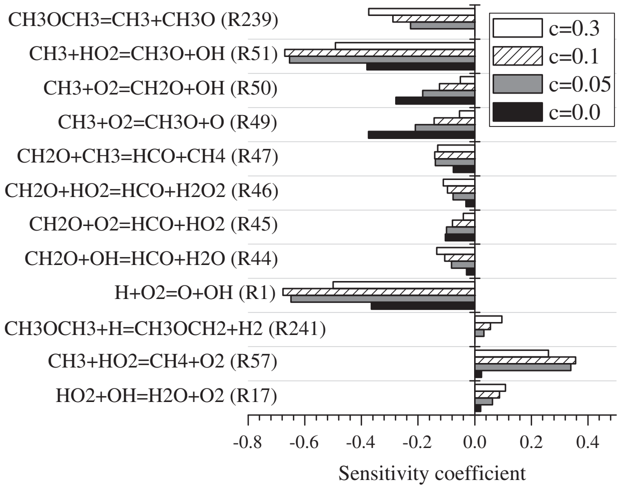

Fig. 5. Sensitivity of key elementary reactions during the homogeneous ignition of stoichiometric CH_4/DME/air at different levels of DME addition.

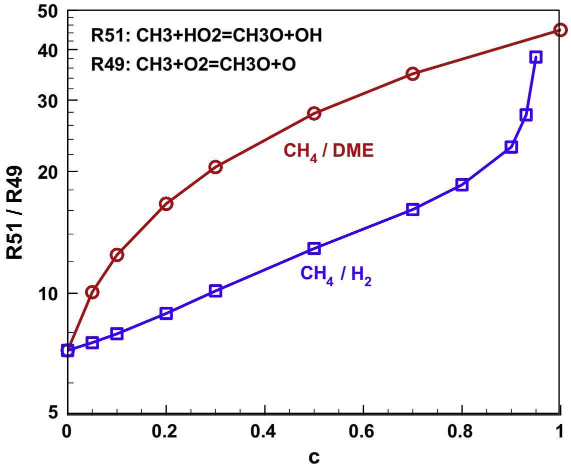

Fig. 6. The ratio of integral CH_3 consumption through reaction R51 to that through reaction R49 in the homogeneous ignition of stoichiometric CH_4/H_2/air and CH_4/DME/air mixtures.

The above results show that both H_2 addition and DME addition can promote the ignition of CH_4. However, different enhancing trends are observed for these two additives. This is due to the fact that different kinetics is involved in the ignition enhancement. When H_2 is added, highly active radicals such as H and OH are produced abundantly via chain reactions R1–R3, leading to a rapid radical build-up and to the transition from slow CH_4-oxidation path to fast H_2-oxidation path. On the other hand, when DME is added, the unimolecular decomposition of DME (R239) amplifies the production of radicals and leads to a large concentration of HO_2, which boosts fast methyl oxidation reaction through reaction R51 that replaces the slower oxidation one, R49.

4. The non-premixed ignition process

In practical combustion processes, ignition is also affected by mixing of fuel and air as well as heat conduction. Since the mass diffusivity of H_2 is about five times larger than that of DME, it is expected that the ignition enhancement by these two additives is different due to transport effects. In order to examine the transport effects involved in CH_4 ignition enhancement by H_2 and DME addition, we study the non-premixed ignition in counterflow configuration. The ignition delay time in the non-premixed counterflow ignition is defined as the time when the maximum temperature in the whole domain is 400 K above the initial temperature of the counter flowing hot air (i.e. $T_{max} = T_{air} + 400\ K = 1800\ K$).

Fig. 7 plots the non-premixed ignition delay time as a function of H_2 and DME blending ratio at three different strain rates. The results for homogeneous ignition are also presented in Fig. 7 for comparison. It is observed that H_2 addition is always more effective than DME addition in terms of promoting the non-premixed ignition of CH_4 with hot air, which is totally different from the homogenous ignition shown in Fig. 1. Fig. 7 shows that the ignition delay time in the non-premixed counterflow configuration differs significantly from that in the homogeneous configuration. When the H_2 blending ratio is in the range of $0.02 < c < 0.8$, the non-premixed ignition is shown to be faster than the homogeneous one. This is counterintuitive since for the transient ignition kernel in the counterflow configuration, there are radical and heat losses due to convective and diffusive transport processes which are unfavorable for ignition. This counterintuitive observation will be explained later.

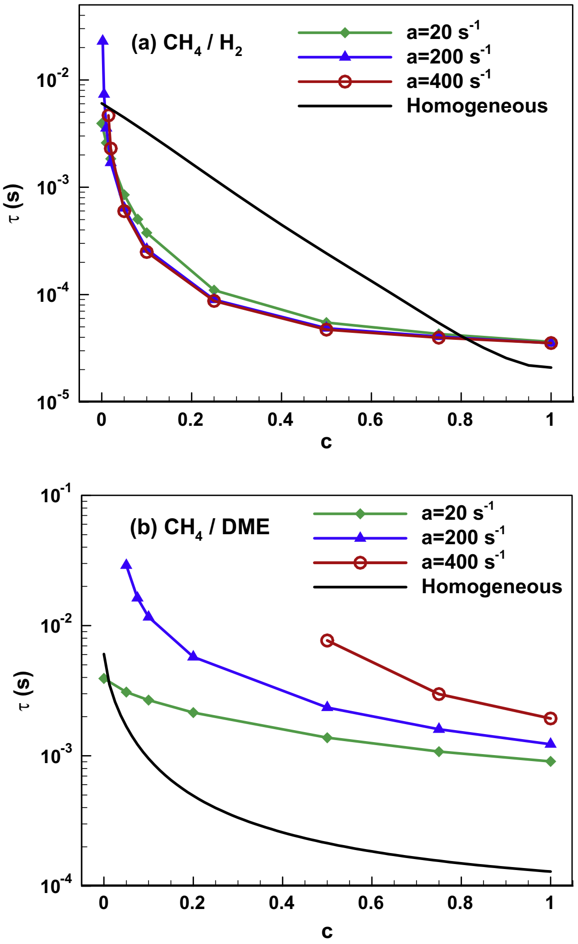

Fig. 7. Chang of the ignition delay time of (a) CH_4/H_2 and (b) CH_4/DME blends in non-premixed counterflow configuration with the H_2 and DME blending ratio in the fuel jet.

Fig. 7a indicates that ignition delay time of CH_4/H_2 mixtures is insensitive to strain rate when $c > 0.05$. This is consistent with the analysis of ignition limits of H_2 in the non-premixed counterflow configuration conducted by Kreutz and Law [21]. They found that the ignition temperature at the second ignition limit of H_2 is insensitive to the strain rate since the ignition process is mainly controlled by kinetics rather than mass and heat transport. The second ignition limit in Ref. [21] covers the conditions in terms of temperature, pressure, and strain rates employed in the present study. Furthermore, as shown later, a small amount of H_2 addition into CH_4 in non-premixed counterflow configuration converts the ignition behavior of CH_4/H_2 blends into the one which is very similar to that of H_2. Therefore, under the conditions considered here, the non-premixed ignition of CH_4/H_2 with $c > 0.05$ is insensitive to the strain rate.

The ignition enhancement by DME addition in counterflow configuration shown in Fig. 7b is quite different from that by H_2 addition in Fig. 7a. For CH_4/DME blends, the ignition delay time in counterflow configuration is always larger than that in homogeneous configuration except the case for very low strain rate ($a = 20\ s^{-1}$) and low DME blending ratio ($c < 0.01$). Furthermore, the strain rate has significant influence on the ignition delay time in the whole range of DME blending ratio. With the increase of strain rate, the ignition delay time increases significantly and the ignition enhancement by DME addition is amplified. This is understandable in view of the fact that at a high strain rate, the short flow residence time prevents the radical pool from quickly building up and thereby DME addition can significantly improve the radical pool build-up through kinetics discussed in the previous section and lead to a strong ignition enhancement at high strain rates [5].

The different behavior shown in Fig. 7 for the non-premixed ignition of CH_4/H_2 and CH_4/DME binary fuel blends is caused by the preferential mass diffusion between CH_4 and H_2 and that between CH_4 and DME. In the above discussion, the blending ratio, c, is defined at the boundary. Here we introduce the local blending ratio at the initial ignition kernel, c_k (i.e., the local molar ratio of H_2 or DME to CH_4 is c_k:$(1 - c_k)$), in the non-premixed counterflow configuration. The initial ignition kernel here is defined as the location of maximum heat release rate immediately after the exothermic process begins following endothermic pyrolysis of fuel. Since the molecular weight of H_2/DME is much smaller/larger than that of CH_4, the mass diffusivity of H_2/DME is much larger/smaller than that of CH_4. In the non-premixed counterflow configuration, ignition starts at the hot air side and fuels need diffuse across the stagnation surface [5,20,26]. Therefore, the preferential mass diffusion between different fuels determines the local blending ratio of H_2 and DME at the ignition kernel. Fig. 8 plots the local blending ratio at the initial ignition kernel, c_k, versus the blending ratio at the boundary, c. Moreover, the results with the mass diffusivity of H_2 and DME artificially modified to the value of CH_4 are presented for comparison. It is observed that the local H_2/DME blending ratio at ignition kernel is in fact much higher/lower than that at the boundary. This is because H_2/DME has much higher/lower mass diffusivity than CH_4 and hence can more easily/difficultly penetrate into the hot air side. When the mass diffusion coefficients of H_2 and DME is artificially changed to be equal to that of CH_4, the local H_2 and DME blending ratio at the ignition kernel is shown to be the same as that at the boundary. Therefore, the local blending ratio of H_2 or DME at the ignition kernel is strongly affected by the preferential mass diffusion. Furthermore, Fig. 8 shows that the results at $a = 20\ s^{-1}$ are almost the same as those at a higher strain rate of $a = 200\ s^{-1}$, indicating that strain rate has a negligible effect on the local blending ratio, c_k.

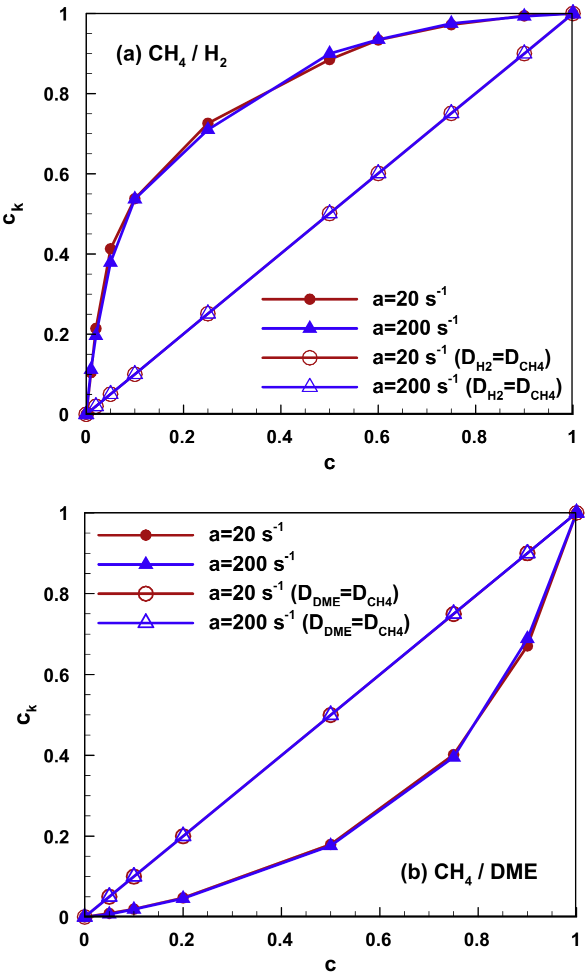

Fig. 8. Comparison between the local blending ratio at the initial ignition kernel with that at the boundary in the fuel jet. The open symbols denote results with the mass diffusion coefficients of (a) H_2 or (b) DME artificially changed to that of CH_4.

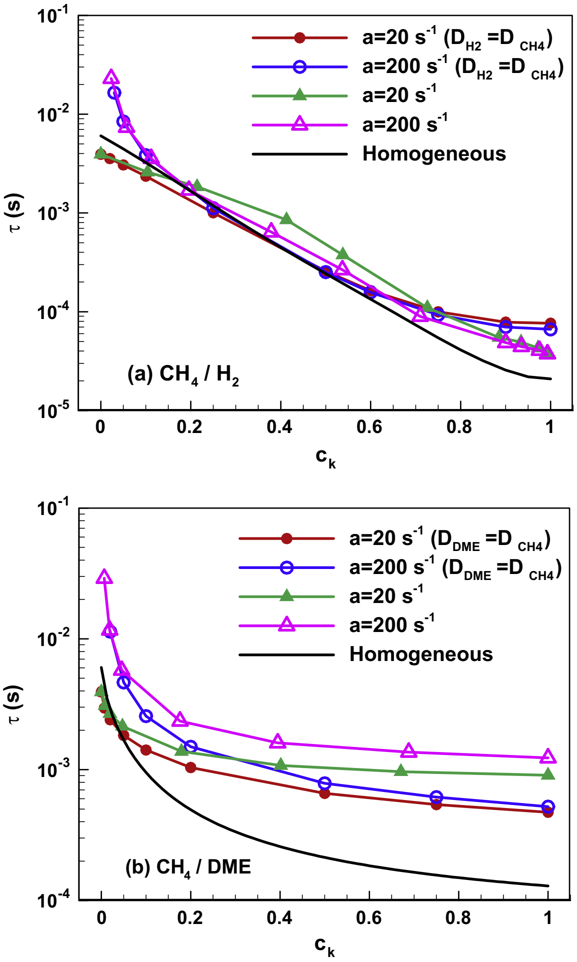

Fig. 9. The ignition delay time of (a) CH_4/H_2 and (b) CH_4/DME blends in non-premixed counterflow configuration as a function of local H_2 and DME blending ratio at the initial ignition kernel.

The influence of preferential mass diffusion on non-premixed ignition is further demonstrated by plotting the ignition delay time as a function of local blending ratio at the ignition kernel in Fig. 9. The results for cases with the mass diffusion coefficients of H_2 and DME artificially changed to that of CH_4 are also plotted in Fig. 9. For H_2 addition, Fig. 9a shows that the results for the non-premixed ignition process are close to those for the homogenous case. Therefore, according to results in Figs. 7, 8 and 9a, the amplification of ignition enhancement by H_2 addition in counterflow configuration is mainly caused by the preferential mass diffusion of H_2 over CH_4 which raises the local H_2 blending ratio at the ignition kernel. However, unlike H_2 addition, Fig 9b shows that the non-premixed ignition is still much slower than the homogeneous ignition at the same local DME blending ratio, especially at higher value of c_k, although an obvious reduction of ignition delay time is observed compared to results in Fig. 7b. Therefore, the ignition enhancement

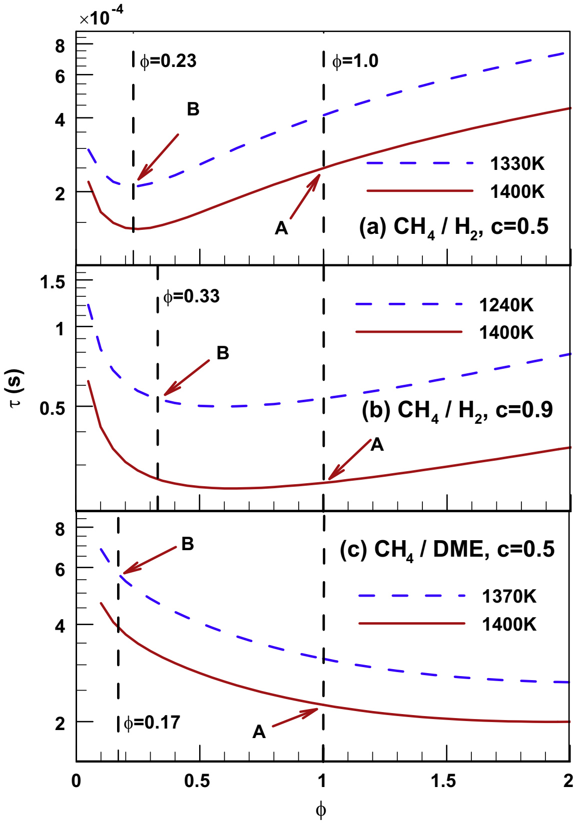

Fig. 10. Change of the homogeneous ignition delay time with the equivalence ratio: (a) CH_4/H_2 with $c = 0.5$; (b) CH_4/H_2 with $c = 0.9$; and (c) CH_4/DME with $c = 0.5$. Points A and B correspond to the initial temperature and equivalence ratio in the homogeneous configuration and the non-premixed counterflow configuration with $a = 200\ s^{-1}$, $D_{H2} = D_{CH4}$ or $D_{DME} = D_{CH4}$, respectively.

by DME addition is only partly reduced by the preferential mass diffusion of CH_4 over DME.

The above analysis indicates that the non-premixed ignition is controlled by the blending ratio at the ignition kernel rather than that in the original fuel jet. The blending ratio at the ignition kernel can significantly differ from that at the boundary if the diffusivities of two fuel components greatly differ from each other.

Fig. 9 shows that in terms of the local blending ratio at the ignition kernel, the ignition delay time for the non-premixed case is close to that for the homogeneous case for CH_4/H_2 binary fuel blends while obvious difference is observed for CH_4/DME binary fuel blends. This is because besides the local blending ratio, other parameters such as local temperature and equivalence ratio at the ignition kernel also affect the ignition. For CH_4/H_2 with $c = 0.5$, the non-premixed ignition delay time with $D_{H2} = D_{CH4}$ is very close to the homogeneous ignition delay time. For the case of $a = 200\ s^{-1}$, $c = 0.5$, and $D_{H2} = D_{CH4}$, the temperature and equivalence ratio at the ignition kernel of counterflow configuration are respectively 1330 K and 0.23, both of which are lower than the values specified in the homogeneous simulation (1400 K and 1.0). Fig. 10 plots the homogeneous ignition delay time as a function of equivalence ratio at different initial temperatures. It is noted that the ignition here is defined as the moment when maximum heat release rate occurs. The total heat release is too small to increase the system by 400 K when the equivalence ratio is very low. Points A and B correspond to the initial temperature and equivalence ratio in the homogeneous configuration and the non-premixed counterflow configuration, respectively. Fig. 10a indicates that due to the coupling influence of initial temperature and equivalence ratio, the ignition delay time at point B is slightly smaller than that at point A. Considering the transport loss in the counterflow configuration, the coincidence of the ignition delay time at $c = 0.5$ in non-premixed counterflow and homogeneous configurations shown in Fig. 9a is reasonable. On the other hand, for $c_k = 0.9$ in Fig. 9a, the ignition delay time in counterflow configuration is much larger than that in homogeneous configuration. This is due to the fact demonstrated in Fig. 10b that the homogeneous ignition delay time at 1400 K is always smaller than that at 1240 K, which is the initial temperature of the ignition kernel in the counterflow configuration with $a = 200\ s^{-1}$.

For CH_4/DME binary fuel blends, Fig. 9b shows that the ignition delay time for the non-premixed case is much larger than that for the homogeneous case. In order to explain this, we chose the case of $c = 0.5$ ($D_{DME} = D_{CH4}$, $a = 200\ s^{-1}$) for further analysis. The initial temperature of the ignition kernel in the counterflow configuration at $c = 0.5$ is around 1370 K and Fig. 10c shows that lean ignition at 1370 K is much slower than the one at point A with $T_u = 1400$ K and $\phi = 1.0$. Therefore, the difference between non-premixed ignition delay time and homogeneous one in Fig. 9b is caused by the influence of temperature and equivalence ratio.

Therefore, the results in Figs. 9 and 10 indicate that the non-premixed ignition counterflow configuration is controlled by not only the local blending ratio but also the local temperature and equivalence ratio at the ignition kernel.

5. Conclusion

The premixed and non-premixed ignition of CH_4/H_2 and CH_4/DME binary fuel blends with air at high temperature and atmospheric pressure is investigated numerically considering detailed chemistry and transport. The kinetic and transport effects involved in CH_4 ignition enhancement by H_2 and DME addition are examined. The main conclusions are as follows:

1. For the homogeneous (premixed) ignition, both H_2 and DME addition can greatly reduce the ignition delay time of CH_4/air mixture. However, different enhancing trends are observed. It is found that when the blending ratio is below 0.53, DME addition is more effective than H_2 addition in terms of promoting the homogeneous ignition of CH_4/air mixture. Sensitivity analysis and reaction path analysis indicate that the kinetics involved in ignition enhancement by H_2 and DME addition are different. When H_2 is added, the chain reactions, $H + O_2 = O + OH$, $O + H_2 = H + OH$, and $H_2 + OH = H_2O + H$ substantially promote radical production and thereby accelerate the ignition process. For DME addition, the unimolecular decomposition of DME and subsequent reactions produce a large amount of HO_2, which in turn promotes the fast reaction $CH_3 + HO_2 = CH_3O + OH$ in competition against the much slower counterpart $CH_3 + O_2 = CH_3O + O$ and thereby greatly accelerate the ignition process.
2. The non-premixed ignition of CH_4/H_2 binary fuel blends is much faster than the homogeneous case and is insensitive to strain rate; while that of the CH_4/DME binary fuel blends is much slower than the homogeneous case and is greatly affected by strain rate. Hydrogen addition is found to be always more effective than DME addition in terms of promoting the non-premixed ignition of CH_4/air mixture. This is due to the facts that the preferential mass diffusion of H_2 over CH_4 significantly raises the local H_2 blending ratio within the ignition kernel and thus amplifies the ignition enhancement; and that on the contrary, the preferential mass diffusion of CH_4 over DME reduces the local DME blending ratio in the ignition kernel and thereby reduces the ignition enhancement. Besides the local blending ratio, the non-premixed ignition in counterflow configuration is also affected by the local temperature and equivalence ratio at the ignition kernel.

Acknowledgments

This work was supported by National Natural Science Foundation of China (Nos. 51322602 and 51136005), Doctoral Fund of Ministry of Education of China (Nos. 20120001110080 and 20100001120003), State Key Laboratory of Engines at Tianjin University (No. K2012-02), and Key Laboratory of Low-grade Energy Utilization Technologies and Systems at Chongqing University (No. LLEUTS 201304).

Appendix A. Supplementary material

Supplementary data associated with this article can be found, in the online version, at http://dx.doi.org/10.1016/j.fuel.2013.10.048.

References

[1] Basic Energy Sciences Workshop, Basic energy needs for clean and efficient combustion of 21st century transportation fuels, US Dept. of Energy; 2007.
[2] Akansu SO, Dulger Z, Kahraman N, Veziroglu TN. Internal combustion engines fueled by natural gas–hydrogen mixtures. Int J Hydrogen Energy 2004;29:1527–39.
[3] Kubesh J, King SR, Liss WE. Effect of gas composition on octane number of natural gas fuels. SAE-922359; 1992.
[4] Karim GA, Wierzba I, AlAlousi Y. Methane–hydrogen mixtures as fuels. Int J Hydrogen Energy 1996;21:625–31.
[5] Chen Z, Qin X, Ju YG, Zhao ZW, Chaos M, Dryer FL. High temperature ignition and combustion enhancement by dimethyl ether addition to methane–air mixtures. Proc Combust Inst 2007;31:1215–22.
[6] Gersen S, Anikin NB, Mokhov AV, Levinsky HB. Ignition properties of methane/hydrogen mixtures in a rapid compression machine. Int J Hydrogen Energy 2008;33:1957–64.
[7] Zhang YJ, Huang ZH, Wei LJ, Zhang JX, Law CK. Experimental and modeling study on ignition delays of lean mixtures of methane, hydrogen, oxygen, and argon at elevated pressures. Combust Flame 2012;159:918–31.
[8] Tang CL, Wei LJ, Zhang JX, Man XJ, Huang ZH. Shock tube measurements and kinetic investigation on the ignition delay times of methane/dimethyl ether mixtures. Energy Fuels 2012;26:6720–8.
[9] Shrestha SOB, Karim GA. Hydrogen as an additive to methane for spark ignition engine applications. Int J Hydrogen Energy 1999;24:577–86.
[10] Bauer CG, Forest TW. Effect of hydrogen addition on the performance of methane-fueled vehicles. Part I: Effect on SI engine performance. Int J Hydrogen Energy 2001;26:55–70.
[11] Wang JH, Chen H, Liu B, Huang ZH. Study of cycle-by-cycle variations of a spark ignition engine fueled with natural gas–hydrogen blends. Int J Hydrogen Energy 2008;33:4876–83.
[12] Ma FH, Wang Y, Liu HQ, Li Y, Wang JJ, Zhao SL. Experimental study on thermal efficiency and emission characteristics of a lean burn hydrogen enriched natural gas engine. Int J Hydrogen Energy 2007;32:5067–75.
[13] Yu G, Law CK, Wu CK. Laminar flame speeds of hydrocarbon + air mixtures with hydrogen addition. Combust Flame 1986;63:339–47.
[14] Huang Z, Zhang Y, Zeng K, Liu B, Wang Q, Jiang DM. Measurements of laminar burning velocities for natural gas–hydrogen–air mixtures. Combust Flame 2006;146:302–11.
[15] Halter F, Chauveau C, Gokalp I. Characterization of the effects of hydrogen addition in premixed methane/air flames. Int J Hydrogen Energy 2007;32:2585–92.
[16] Chen Z. Effects of hydrogen addition on the propagation of spherical methane/air flames: a computational study. Int J Hydrogen Energy 2009;34:6558–67.
[17] Hu EJ, Huang ZH, He JJ, Miao HY. Experimental and numerical study on lean premixed methane–hydrogen–air flames at elevated pressures and temperatures. Int J Hydrogen Energy 2009;34:6951–60.
[18] Zhao ZL, Chen Z. HDMR correlations for the laminar burning velocity of premixed $CH_4/H_2/O_2/N_2$ mixtures. Int J Hydrogen Energy 2012;37:691–7.
[19] Chen Z, Dai P, Chen SY. A model for the laminar flame speed of binary fuel blends and its application to methane/hydrogen mixtures. Int J Hydrogen Energy 2012;37:10390–6.
[20] Dai P, Chen Z, Chen SY. Numerical study on the ignition process of n-decane/toluene binary fuel blends. Energy Fuels 2012;26:6729–36.
[21] Kreutz TG, Law CK. Ignition in nonpremixed counter flowing hydrogen versus heated air: computational study with detailed chemistry. Combust Flame 1996;104:157–75.
[22] Fotache CG, Kreutz TG, Law CK. Ignition of hydrogen-enriched methane by heated air. Combust Flame 1997;110:429–40.
[23] Zheng XL, Blouch JD, Zhu DL, Kreutz TG, Law CK. Ignition of premixed hydrogen/air by heated counterflow. Proc Combust Inst 2002;29:1637–43.
[24] Sun WT, Won SH, Ombrello T, Carter C, Ju YG. Direct ignition and *S*-curve transition by in situ nano-second pulsed discharge in methane/oxygen/helium counterflow flame. Proc Combust Inst 2013;34:847–55.
[25] Ju YG, Guo HS, Maruta K, Liu FS. On the extinction limit and flammability limit of non-adiabatic stretched methane–air premixed flames. J Fluid Mech 1997;342:315–34.
[26] Liu SL, Hewson JC, Chen JH, Pitsch H. Effects of strain rate on high-pressure nonpremixed n-heptane autoignition in counterflow. Combust Flame 2004;137:320–39.
[27] Zhao Z, Chaos M, Kazakov A, Dryer FL. Thermal decomposition reaction and a comprehensive kinetic model of dimethyl ether. Int J Chem Kinet 2008;40:1–18.
[28] Li J, Zhao ZW, Kazakov A, Dryer FL. An updated comprehensive kinetic model of hydrogen combustion. Int J Chem Kinet 2004;36:566–75.
[29] Zhao ZL, Chen Z, Chen SY. Correlations for the ignition delay times of hydrogen/air mixtures. Chin Sci Bull 2011;56:215–21.
[30] Guo P, Chen Z. Ignition enhancement of ethylene/air by NOx addition. Chin J Aeronaut 2013;26:876–83.